

Search for Associated Production of Υ and Vector Boson in $p\bar{p}$ Collisions at $\sqrt{s} = 1.8$ TeV

D. Acosta,¹⁴ T. Affolder,²⁵ H. Akimoto,⁵¹ M. G. Albrow,¹³ D. Ambrose,³⁷ D. Amidei,²⁸ K. Anikeev,²⁷ J. Antos,¹ G. Apollinari,¹³ T. Arisawa,⁵¹ A. Artikov,¹¹ T. Asakawa,⁴⁹ W. Ashmanskas,¹⁰ F. Azfar,³⁵ P. Azzi-Bacchetta,³⁶ N. Bacchetta,³⁶ H. Bachacou,²⁵ W. Badgett,¹³ S. Bailey,¹⁸ P. de Barbaro,⁴¹ A. Barbaro-Galtieri,²⁵ V. E. Barnes,⁴⁰ B. A. Barnett,²¹ S. Baroiant,⁵ M. Barone,¹⁵ G. Bauer,²⁷ F. Bedeschi,³⁸ S. Behari,²¹ S. Belforte,⁴⁸ W. H. Bell,¹⁷ G. Bellettini,³⁸ J. Bellinger,⁵² D. Benjamin,¹² J. Bensinger,⁴ A. Beretvas,¹³ J. Berryhill,¹⁰ A. Bhatti,⁴² M. Binkley,¹³ D. Bisello,³⁶ M. Bishai,¹³ R. E. Blair,² C. Blocker,⁴ K. Bloom,²⁸ B. Blumenfeld,²¹ S. R. Blusk,⁴¹ A. Bocci,⁴² A. Bodek,⁴¹ G. Bolla,⁴⁰ A. Bolshov,²⁷ Y. Bonushkin,⁶ D. Bortoletto,⁴⁰ J. Boudreau,³⁹ A. Brandl,³¹ C. Bromberg,²⁹ M. Brozovic,¹² E. Brubaker,²⁵ N. Bruner,³¹ J. Budagov,¹¹ H. S. Budd,⁴¹ K. Burkett,¹⁸ G. Busetto,³⁶ K. L. Byrum,² S. Cabrera,¹² P. Calafiura,²⁵ M. Campbell,²⁸ W. Carithers,²⁵ J. Carlson,²⁸ D. Carlsmith,⁵² W. Caskey,⁵ A. Castro,³ D. Cauz,⁴⁸ A. Cerri,³⁸ L. Cerrito,²⁰ A. W. Chan,¹ P. S. Chang,¹ P. T. Chang,¹ J. Chapman,²⁸ C. Chen,³⁷ Y. C. Chen,¹ M.-T. Cheng,¹ M. Chertok,⁵ G. Chiarelli,³⁸ I. Chirikov-Zorin,¹¹ G. Chlachidze,¹¹ F. Chlebana,¹³ L. Christofek,²⁰ M. L. Chu,¹ J. Y. Chung,³³ W.-H. Chung,⁵² Y. S. Chung,⁴¹ C. I. Ciobanu,³³ A. G. Clark,¹⁶ M. Coca,⁴¹ A. P. Colijn,¹³ A. Connolly,²⁵ M. Convery,⁴² J. Conway,⁴⁴ M. Cordelli,¹⁵ J. Cranshaw,⁴⁶ R. Culbertson,¹³ D. Dagenhart,⁴ S. D'Auria,¹⁷ S. De Cecco,⁴³ F. DeJongh,¹³ S. Dell'Agnello,¹⁵ M. Dell'Orso,³⁸ S. Demers,⁴¹ L. Demortier,⁴² M. Deninno,³ D. De Pedis,⁴³ P. F. Derwent,¹³ T. Devlin,⁴⁴ C. Dionisi,⁴³ J. R. Dittmann,¹³ A. Dominguez,²⁵ S. Donati,³⁸ M. D'Onofrio,³⁸ T. Dorigo,³⁶ N. Eddy,²⁰ K. Einsweiler,²⁵ E. Engels, Jr.,³⁹ R. Erbacher,¹³ D. Errede,²⁰ S. Errede,²⁰ R. Eusebi,⁴¹ Q. Fan,⁴¹ H.-C. Fang,²⁵ S. Farrington,¹⁷ R. G. Feild,⁵³ J. P. Fernandez,⁴⁰ C. Ferretti,²⁸ R. D. Field,¹⁴ I. Fiori,³ B. Flaughner,¹³ L. R. Flores-Castillo,³⁹ G. W. Foster,¹³ M. Franklin,¹⁸ J. Freeman,¹³ J. Friedman,²⁷ Y. Fukui,²³ I. Furic,²⁷ S. Galeotti,³⁸ A. Gallas,³² M. Gallinaro,⁴² T. Gao,³⁷ M. Garcia-Sciveres,²⁵ A. F. Garfinkel,⁴⁰ P. Gatti,³⁶ C. Gay,⁵³ D. W. Gerdes,²⁸ E. Gerstein,⁹ S. Giagu,⁴³ P. Giannetti,³⁸ K. Giolo,⁴⁰ M. Giordani,⁵ P. Giromini,¹⁵ V. Glagolev,¹¹ D. Glenzinski,¹³ M. Gold,³¹ N. Goldschmidt,²⁸ J. Goldstein,¹³ G. Gomez,⁸ M. Goncharov,⁴⁵ I. Gorelov,³¹ A. T. Goshaw,¹² Y. Gotra,³⁹ K. Goulianos,⁴² C. Green,⁴⁰ A. Gresele,³⁶ G. Grim,⁵ C. Grosso-Pilcher,¹⁰ M. Guenther,⁴⁰ G. Guillian,²⁸ J. Guimaraes da Costa,¹⁸ R. M. Haas,¹⁴ C. Haber,²⁵ S. R. Hahn,¹³ E. Halkiadakis,⁴¹ C. Hall,¹⁸ T. Handa,¹⁹ R. Handler,⁵² F. Happacher,¹⁵ K. Hara,⁴⁹ A. D. Hardman,⁴⁰ R. M. Harris,¹³ F. Hartmann,²² K. Hatakeyama,⁴² J. Hauser,⁶ J. Heinrich,³⁷ A. Heiss,²² M. Hennecke,²² M. Herndon,²¹ C. Hill,⁷ A. Hocker,⁴¹ K. D. Hoffman,¹⁰ R. Hollebeek,³⁷ L. Holloway,²⁰ S. Hou,¹ B. T. Huffman,³⁵ R. Hughes,³³ J. Huston,²⁹ J. Huth,¹⁸ H. Ikeda,⁴⁹ J. Incandela,⁷ G. Introzzi,³⁸ M. Iori,⁴³ A. Ivanov,⁴¹ J. Iwai,⁵¹ Y. Iwata,¹⁹ B. Iyutin,²⁷ E. James,²⁸ M. Jones,³⁷ U. Joshi,¹³ H. Kambara,¹⁶ T. Kamon,⁴⁵ T. Kaneko,⁴⁹ J. Kang,²⁸ M. Karagoz Unel,³² K. Karr,⁵⁰ S. Kartal,¹³ H. Kasha,⁵³ Y. Kato,³⁴ T. A. Keaffaber,⁴⁰ K. Kelley,²⁷ M. Kelly,²⁷ R. D. Kennedy,¹³ R. Kephart,¹³ D. Khazins,¹² T. Kikuchi,⁴⁹ B. Kilminster,⁴¹ B. J. Kim,²⁴ D. H. Kim,²⁴ H. S. Kim,²⁰ M. J. Kim,⁹ S. B. Kim,²⁴ S. H. Kim,⁴⁹ T. H. Kim,²⁷ Y. K. Kim,²⁵ M. Kirby,¹² M. Kirk,⁴ L. Kirsch,⁴ S. Klimenko,¹⁴ P. Koehn,³³ K. Kondo,⁵¹ J. Konigsberg,¹⁴ A. Korn,²⁷ A. Korytov,¹⁴ K. Kotelnikov,³⁰ E. Kovacs,² J. Kroll,³⁷ M. Kruse,¹² V. Krutelyov,⁴⁵ S. E. Kuhlmann,² K. Kurino,¹⁹ T. Kuwabara,⁴⁹ N. Kuznetsova,¹³ A. T. Laasanen,⁴⁰ K. W. Lai,^{54,*} N. Lai,¹⁰ S. Lami,⁴² S. Lammel,¹³ J. Lancaster,¹² K. Lannon,²⁰ M. Lancaster,²⁶ R. Lander,⁵ A. Lath,⁴⁴ G. Latino,³¹ T. LeCompte,² Y. Le,²¹ J. Lee,⁴¹ S. W. Lee,⁴⁵ N. Leonardo,²⁷ S. Leone,³⁸ J. D. Lewis,¹³ K. Li,⁵³ C. S. Lin,¹³ M. Lindgren,⁶ T. M. Liss,²⁰ J. B. Liu,⁴¹ T. Liu,¹³ Y. C. Liu,¹ D. O. Litvintsev,¹³ O. Lobban,⁴⁶ N. S. Lockyer,³⁷ A. Loginov,³⁰ J. Loken,³⁵ M. Loretì,³⁶ D. Lucchesi,³⁶ P. Lukens,¹³ S. Lusin,⁵² L. Lyons,³⁵ J. Lys,²⁵ R. Madrak,¹⁸ K. Maeshima,¹³ P. Maksimovic,²¹ L. Malferrari,³ M. Mangano,³⁸ G. Manca,³⁵ M. Mariotti,³⁶ G. Martignon,³⁶ M. Martin,²¹ A. Martin,⁵³ V. Martin,³² J. A. J. Matthews,³¹ P. Mazzanti,³ K. S. McFarland,⁴¹ P. McIntyre,⁴⁵ M. Menguzzato,³⁶ A. Menzione,³⁸ P. Merkel,¹³ C. Mesropian,⁴² A. Meyer,¹³ T. Miao,¹³ R. Miller,²⁹ J. S. Miller,²⁸ H. Minato,⁴⁹ S. Miscetti,¹⁵ M. Mishina,²³ G. Mitselmakher,¹⁴ Y. Miyazaki,³⁴ N. Moggi,³ E. Moore,³¹ R. Moore,²⁸ Y. Morita,²³ T. Moulik,⁴⁰ M. Mulhearn,²⁷ A. Mukherjee,¹³ T. Muller,²² A. Munar,³⁸ P. Murat,¹³ S. Murgia,²⁹ J. Nachtman,⁶ V. Nagaslaev,⁴⁶ S. Nahn,⁵³ H. Nakada,⁴⁹ I. Nakano,¹⁹ R. Naporá,²¹ F. Niell,²⁸ C. Nelson,¹³ T. Nelson,¹³ C. Neu,³³ M. S. Neubauer,²⁷ D. Neuberger,²² C. Newman-Holmes,¹³ C.-Y. P. Ngan,²⁷ T. Nigmanov,³⁹ H. Niu,⁴ L. Nodulman,² A. Nomerotski,¹⁴ S. H. Oh,¹² Y. D. Oh,²⁴ T. Ohmoto,¹⁹ T. Ohsugi,¹⁹ R. Oishi,⁴⁹ T. Okusawa,³⁴ J. Olsen,⁵² W. Orejudos,²⁵ C. Pagliarone,³⁸ F. Palmonari,³⁸ R. Paoletti,³⁸ V. Papadimitriou,⁴⁶ D. Partos,⁴ J. Patrick,¹³ G. Pauletta,⁴⁸ M. Paulini,⁹ T. Pauly,³⁵ C. Paus,²⁷ D. Pellett,⁵ A. Penzo,⁴⁸ L. Pescara,³⁶ T. J. Phillips,¹² G. Piacentino,³⁸ J. Piedra,⁸ K. T. Pitts,²⁰ A. Pompoš,⁴⁰ L. Pondrom,⁵² G. Pope,³⁹ T. Pratt,³⁵ F. Prokoshin,¹¹ J. Proudfoot,² F. Ptohos,¹⁵ O. Pukhov,¹¹ G. Punzi,³⁸ J. Rademacker,³⁵ A. Rakitine,²⁷ F. Ratnikov,⁴⁴ H. Ray,²⁸ D. Reher,²⁵ A. Reichold,³⁵ P. Renton,³⁵ M. Rescigno,⁴³ A. Ribon,³⁶ W. Riegler,¹⁸ F. Rimondi,³ L. Ristori,³⁸ M. Rivelino,⁴⁷ W. J. Robertson,¹² T. Rodrigo,⁸

S. Rolli,⁵⁰ L. Rosenson,²⁷ R. Roser,¹³ R. Rossin,³⁶ C. Rott,⁴⁰ A. Roy,⁴⁰ A. Ruiz,⁸ D. Ryan,⁵⁰ A. Safonov,⁵ R. St. Denis,¹⁷ W. K. Sakumoto,⁴¹ D. Saltzberg,⁶ C. Sanchez,³³ A. Sansoni,¹⁵ L. Santi,⁴⁸ S. Sarkar,⁴³ H. Sato,⁴⁹ P. Savard,⁴⁷ A. Savoy-Navarro,¹³ P. Schlabach,¹³ E. E. Schmidt,¹³ M. P. Schmidt,⁵³ M. Schmitt,³² L. Scodellaro,³⁶ A. Scott,⁶ A. Scribano,³⁸ A. Sedov,⁴⁰ S. Seidel,³¹ Y. Seiya,⁴⁹ A. Semenov,¹¹ F. Semeria,³ T. Shah,²⁷ M. D. Shapiro,²⁵ P. F. Shepard,³⁹ T. Shibayama,⁴⁹ M. Shimojima,⁴⁹ M. Shochet,¹⁰ A. Sidoti,³⁶ J. Siegrist,²⁵ A. Sill,⁴⁶ P. Sinervo,⁴⁷ P. Singh,²⁰ A. J. Slaughter,⁵³ K. Sliwa,⁵⁰ F. D. Snider,¹³ R. Snihur,²⁶ A. Solodsky,⁴² J. Spalding,¹³ T. Speer,¹⁶ M. Spezziga,⁴⁶ P. Sphicas,²⁷ F. Spinella,³⁸ M. Spiropulu,¹⁰ L. Spiegel,¹³ J. Steele,⁵² A. Stefanini,³⁸ J. Strologas,²⁰ F. Strumia,¹⁶ D. Stuart,⁷ A. Sukhanov,¹⁴ K. Sumorok,²⁷ T. Suzuki,⁴⁹ T. Takano,³⁴ R. Takashima,¹⁹ K. Takikawa,⁴⁹ P. Tamburello,¹² M. Tanaka,⁴⁹ B. Tannenbaum,⁶ M. Tecchio,²⁸ R. J. Tesarek,¹³ P. K. Teng,¹ K. Terashi,⁴² S. Tether,²⁷ A. S. Thompson,¹⁷ E. Thomson,³³ R. Thurman-Keup,² P. Tipton,⁴¹ S. Tkaczyk,¹³ D. Toback,⁴⁵ K. Tollefson,²⁹ D. Tonelli,³⁸ M. Tonnesmann,²⁹ H. Toyoda,³⁴ W. Trischuk,⁴⁷ J. F. de Troconiz,¹⁸ J. Tseng,²⁷ D. Tsybychev,¹⁴ N. Turini,³⁸ F. Ukegawa,⁴⁹ T. Unverhau,¹⁷ T. Vaiciulis,⁴¹ J. Valls,⁴⁴ A. Varganov,²⁸ E. Vataga,³⁸ S. Vajc III,¹³ G. Velev,¹³ G. Veramendi,²⁵ R. Vidal,¹³ I. Vila,⁸ R. Vilar,⁸ I. Volobouev,²⁵ M. von der Mey,⁶ D. Vucinic,²⁷ R. G. Wagner,² R. L. Wagner,¹³ W. Wagner,²² N. B. Wallace,⁴⁴ Z. Wan,⁴⁴ C. Wang,¹² M. J. Wang,¹ S. M. Wang,¹⁴ B. Ward,¹⁷ S. Waschke,¹⁷ T. Watanabe,⁴⁹ D. Waters,²⁶ T. Watts,⁴⁴ M. Weber,²⁵ H. Wenzel,²² W. C. Wester III,¹³ B. Whitehouse,⁵⁰ A. B. Wicklund,² E. Wicklund,¹³ T. Wilkes,⁵ H. H. Williams,³⁷ P. Wilson,¹³ B. L. Winer,³³ D. Winn,²⁸ S. Wolbers,¹³ D. Wolinski,²⁸ J. Wolinski,²⁹ S. Wolinski,²⁸ M. Wolter,⁵⁰ S. Worm,⁴⁴ X. Wu,¹⁶ F. Würthwein,²⁷ J. Wyss,³⁸ U. K. Yang,¹⁰ W. Yao,²⁵ G. P. Yeh,¹³ P. Yeh,¹ K. Yi,²¹ J. Yoh,¹³ C. Yosef,²⁹ T. Yoshida,³⁴ I. Yu,²⁴ S. Yu,³⁷ Z. Yu,⁵³ J. C. Yun,¹³ L. Zanello,⁴³ A. Zanetti,⁴⁸ F. Zetti,²⁵ and S. Zucchelli³

(CDF Collaboration)

¹*Institute of Physics, Academia Sinica, Taipei, Taiwan 11529, Republic of China*

²*Argonne National Laboratory, Argonne, Illinois 60439, USA*

³*Istituto Nazionale di Fisica Nucleare, University of Bologna, I-40127 Bologna, Italy*

⁴*Brandeis University, Waltham, Massachusetts 02254, USA*

⁵*University of California at Davis, Davis, California 95616, USA*

⁶*University of California at Los Angeles, Los Angeles, California 90024, USA*

⁷*University of California at Santa Barbara, Santa Barbara, California 93106, USA*

⁸*Instituto de Fisica de Cantabria, CSIC-University of Cantabria, 39005 Santander, Spain*

⁹*Carnegie Mellon University, Pittsburgh, Pennsylvania 15218, USA*

¹⁰*Enrico Fermi Institute, University of Chicago, Chicago, Illinois 60637, USA*

¹¹*Joint Institute for Nuclear Research, RU-141980 Dubna, Russia*

¹²*Duke University, Durham, North Carolina 27708, USA*

¹³*Fermi National Accelerator Laboratory, Batavia, Illinois 60510, USA*

¹⁴*University of Florida, Gainesville, Florida 32611, USA*

¹⁵*Laboratori Nazionali di Frascati, Istituto Nazionale di Fisica Nucleare, I-00044 Frascati, Italy*

¹⁶*University of Geneva, CH-1211 Geneva 4, Switzerland*

¹⁷*Glasgow University, Glasgow G12 8QQ, United Kingdom*

¹⁸*Harvard University, Cambridge, Massachusetts 02138, USA*

¹⁹*Hiroshima University, Higashi-Hiroshima 724, Japan*

²⁰*University of Illinois, Urbana, Illinois 61801, USA*

²¹*The Johns Hopkins University, Baltimore, Maryland 21218, USA*

²²*Institut für Experimentelle Kernphysik, Universität Karlsruhe, 76128 Karlsruhe, Germany*

²³*High Energy Accelerator Research Organization (KEK), Tsukuba, Ibaraki 305, Japan*

²⁴*Center for High Energy Physics, Kyungpook National University, Taegu 702-701; Seoul National University, Seoul 151-742; and Sungkyunkwan University, Suwon 440-746; Korea*

²⁵*Ernest Orlando Lawrence Berkeley National Laboratory, Berkeley, California 94720, USA*

²⁶*University College London, London WC1E 6BT, United Kingdom*

²⁷*Massachusetts Institute of Technology, Cambridge, Massachusetts 02139, USA*

²⁸*University of Michigan, Ann Arbor, Michigan 48109, USA*

²⁹*Michigan State University, East Lansing, Michigan 48824, USA*

³⁰*Institution for Theoretical and Experimental Physics, ITEP, Moscow 117259, Russia*

³¹*University of New Mexico, Albuquerque, New Mexico 87131, USA*

³²*Northwestern University, Evanston, Illinois 60208, USA*

³³*The Ohio State University, Columbus, Ohio 43210, USA*

³⁴*Osaka City University, Osaka 588, Japan*

³⁵*University of Oxford, Oxford OX1 3RH, United Kingdom*

- ³⁶*Universita di Padova, Istituto Nazionale di Fisica Nucleare, Sezione di Padova, I-35131 Padova, Italy*
- ³⁷*University of Pennsylvania, Philadelphia, Pennsylvania 19104, USA*
- ³⁸*Istituto Nazionale di Fisica Nucleare, University and Scuola Normale Superiore of Pisa, I-56100 Pisa, Italy*
- ³⁹*University of Pittsburgh, Pittsburgh, Pennsylvania 15260, USA*
- ⁴⁰*Purdue University, West Lafayette, Indiana 47907, USA*
- ⁴¹*University of Rochester, Rochester, New York 14627, USA*
- ⁴²*Rockefeller University, New York, New York 10021, USA*
- ⁴³*Istituto Nazionale de Fisica Nucleare, Sezione di Roma, University di Roma I, "La Sapienza," I-00185 Roma, Italy*
- ⁴⁴*Rutgers University, Piscataway, New Jersey 08855, USA*
- ⁴⁵*Texas A&M University, College Station, Texas 77843, USA*
- ⁴⁶*Texas Tech University, Lubbock, Texas 79409, USA*
- ⁴⁷*Institute of Particle Physics, University of Toronto, Toronto M5S 1A7, Canada*
- ⁴⁸*Istituto Nazionale di Fisica Nucleare, University of Trieste, Udine, Italy*
- ⁴⁹*University of Tsukuba, Tsukuba, Ibaraki 305, Japan*
- ⁵⁰*Tufts University, Medford, Massachusetts 02155, USA*
- ⁵¹*Waseda University, Tokyo 169, Japan*
- ⁵²*University of Wisconsin, Madison, Wisconsin 53706, USA*
- ⁵³*Yale University, New Haven, Connecticut 06520, USA*
- ⁵⁴*Universita' di Padova, Istituto Nazionale di Fisica Nucleare, Sezione di Padova, I-35131 Padova, Italy*
(Received 9 December 2002; published 6 June 2003)

We present a search for associated production of the $Y(1S)$ and a vector boson in 83 pb^{-1} of $p\bar{p}$ collisions at $\sqrt{s} = 1.8 \text{ TeV}$ collected by the CDF experiment in 1994–1995. We find no evidence of the searched signal in the data, and set upper limits to the production cross sections.

DOI: 10.1103/PhysRevLett.90.221803

PACS numbers: 13.20.Gd, 13.85.Rm, 14.70.Fm, 14.70.Hp

The production of Y mesons associated with vector bosons was examined in a recent paper [1], where expectations at the Tevatron $p\bar{p}$ collider in the standard model (SM) framework were given. The cross section estimates of Ref. [1] for $\sqrt{s} = 1.8 \text{ TeV}$ are of the order of 0.47 and 0.18 pb for $Y(1S)W$ and $Y(1S)Z$ production, respectively. In the context of supersymmetric models (SUSY), a charged Higgs boson lighter than about $180 \text{ GeV}/c^2$ can have a sizable branching ratio into YW pairs if the ratio of vacuum expectation values $\tan(\beta)$ is small, and similarly a light neutral scalar can decay to YZ pairs [2]. Although the rates of the SM decays are predicted to be too small to be observable at the Tevatron with currently available statistics, model uncertainties are large, and a search for these processes in the present data, which has never been performed before, is useful for extrapolations to future searches in the SUSY sector.

The main SM production mechanism proceeds through the creation of a vector boson together with a $b\bar{b}$ pair which binds to form a $Y(1S)$. The process is described by nonperturbative matrix elements based on the relative velocity of the b quarks in the pair; the formation of a $b\bar{b}$ pair has been considered both in color singlet and octet configurations [3]. Additional contributions to the $Y(1S)$ signal due to the feed-down from higher bottomonium states, mainly $Y(2S)$ and $Y(3S)$, account for $\approx 20\%$ of the total production [1].

The data used in this analysis were collected by CDF during the 1994–1995 run of the Tevatron collider, and correspond to an integrated luminosity of $\int \mathcal{L} dt = 83.4 \pm 3.4 \text{ pb}^{-1}$.

The CDF detector has been described in detail elsewhere [4]. We briefly describe here the portions of the detector used in this analysis. CDF consists of a magnetic spectrometer surrounded by calorimeters and muon chambers. The momenta of charged particles are measured out to a pseudorapidity [5] of $|\eta| < 1.1$ in the central tracking chamber (CTC), which is inside a 1.4 T superconducting solenoidal magnet. The silicon microstrip vertex detector (SVX) [6], located immediately outside the beam pipe, provides precise track reconstruction in the plane transverse to the beam. Energy and direction of electrons, photons, and jets are measured by three calorimeter systems covering the central ($|\eta| < 1.1$), intermediate ($1.1 < |\eta| < 2.4$), and forward ($|\eta| > 2.4$) regions; each calorimeter has an electromagnetic (EM) and a hadronic (HAD) section. The central muon detection system (CMU) consists of drift chambers located outside the calorimeter, allowing the reconstruction of track segments for penetrating particles. An additional set of chambers (CMP) instrumented with scintillation counters is located outside a 0.6 m thick iron wall, providing additional discrimination against punch-through hadrons. Muons with $0.6 < |\eta| < 1.0$ are detected by another set of drift chambers (CMX) sandwiched between scintillation counters. Y mesons are thus easily identified through their decay to $\mu^+\mu^-$ pairs, while vector bosons are selected via their decay to leptons or to jets of hadrons. The present search focuses on the identification of the $Y(1S)$ state only due to the lower branching fraction of the $Y(2S)$ and $Y(3S)$ to the $\mu^+\mu^-$ final state and to their sizable feed-down to the $(1S)$ state.

The samples of data used in this analysis were collected by means of two different three-level muon triggers. The first was a dimuon trigger that selected events with two tracks detected in the CMU chambers with transverse momentum $P_T > 2.2$ GeV/ c as measured by the Central Fast Tracker (CFT), a hardware track processor with a momentum resolution of $\delta P_T/P_T^2 = 0.03$ (GeV/ c) $^{-1}$. At least one of the muons had to be detected also in the CMP chambers. The second trigger was used to identify single muon candidates. It required that a track segment found at Level 1 in the CMU and CMP detectors matched a CFT track with $P_T > 7.5$ GeV/ c .

Offline muon identification started with the requirement that the energy deposited in the calorimeter by the candidate be consistent with that of a minimum ionizing particle: we required $E_T^{EM} < 1$ GeV in the electromagnetic section, $E_T^{HAD} < 4$ GeV in the hadronic section, and $E_T^{EM} + E_T^{HAD} > 0.1$ GeV. Pairs of opposite-charge muon tracks are required to have a difference in z coordinates at the point of closest approach to the beam axis within 5 cm. To further reduce fake muon backgrounds, an optimized selection was performed using the χ^2 of the three-dimensional match of the CTC track with the segment in the muon chambers. In addition, the impact parameter significance of muon tracks reconstructed by the SVX was used to get rid also of heavy flavor semi-leptonic decays, enhancing the prompt Υ production of muons. The invariant mass of muon pairs was required to be in the 8 to 12 GeV/ c^2 range. Figure 1 shows the resulting dimuon mass spectrum. We estimate the number of events due to $\Upsilon(1S)$ production to be 5143 ± 96 .

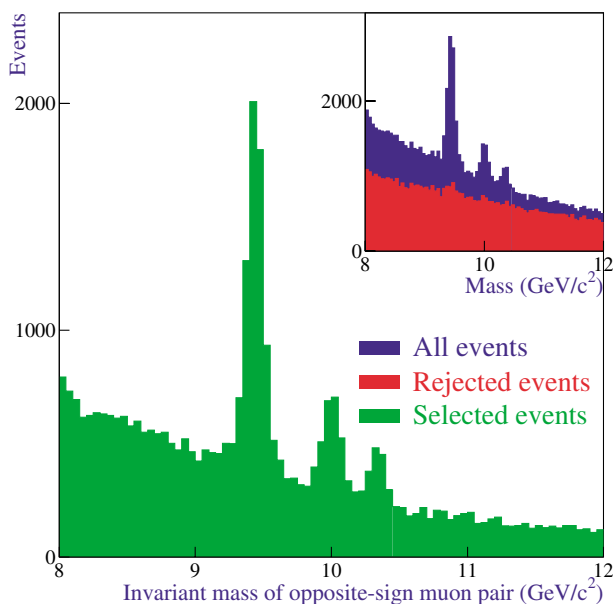


FIG. 1 (color online). Invariant mass of the two opposite-charge muons before (inset) and after (full-scale histogram) the selection of good muon pairs described in the text.

The Herwig generator [7] was used to generate $\Upsilon(1S) +$ vector boson events. The P_T differential cross sections for the hard production processes of $\Upsilon(1S)W^\pm$ and $\Upsilon(1S)Z^0$ were supplied by the authors of Ref. [1] and introduced into the generator. The $\Upsilon(1S)$ was forced to decay to $\mu^+\mu^-$. A detailed simulation of the CDF detector and a full reconstruction were applied to the events, which were then filtered using a simulation of the dimuon and single muon trigger conditions.

Υ mesons produced in association with vector bosons are characterized by a high P_T with respect to other production processes, as shown in Fig. 2. Therefore, events with $P_T(\mu\mu) > 5$ GeV/ c were selected.

The search for a signal of vector boson decay in the selected data was performed using four independent experimental signatures: the detection of high- E_T electrons, high- P_T muons, significant missing transverse energy (\cancel{E}_T), or pairs of hadronic jets. The \cancel{E}_T constitutes an independent signal of $W^\pm \rightarrow \tau\nu$ or $Z^0 \rightarrow \nu\bar{\nu}$ decays, as well as a tag of W^\pm decays to unidentified electrons or muons.

In order to have maximum sensitivity to the searched signal the selection of electrons and muons was looser than that normally used for the collection of W and Z bosons at CDF [8]. Electron candidates were selected by requiring an electromagnetic cluster in the calorimeter with $E_T > 20$ GeV, limiting the energy deposited in the hadronic section by $E^{HAD}/E^{EM} < 0.05$, and associating a reconstructed track in the CTC with $P_T > 10$ GeV/ c that satisfies $E/P < 1.8$. Muon candidates must have $P_T > 20$ GeV/ c and an energy deposit in the

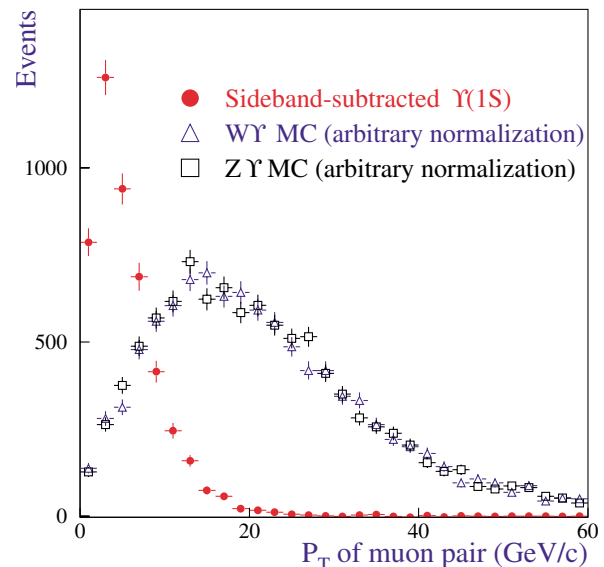


FIG. 2 (color online). Transverse momentum of background-subtracted $\Upsilon(1S)$ candidates in the data (full circles) compared to $\Upsilon(1S)$ mesons from the SM simulation of $\Upsilon(1S)W^\pm$ and $\Upsilon(1S)Z^0$ production (empty triangles and squares), with arbitrary normalization.

calorimeter consistent with that produced by minimum ionizing particles, as described for the Y -decay muons above.

The presence of undetected high- P_T neutrinos was inferred by the significance of missing transverse energy $s = \cancel{E}_T / \sigma_{\cancel{E}_T} > 3$, where \cancel{E}_T and $\sigma_{\cancel{E}_T} \sim 100\% \sqrt{\sum E_T} / \text{GeV}$ were computed using all calorimeter towers with $|\eta| < 3.6$. The missing E_T was also corrected for the presence of minimum ionizing particles and mismeasured jets.

Hadronic jets were reconstructed with a $\Delta R = \sqrt{\Delta\phi^2 + \Delta\eta^2} = 0.4$ cone algorithm and selected if they had measured $E_T > 10$ GeV and $|\eta| < 2.0$. The energy of the two leading jets was then corrected for calorimeter nonlinearities, energy deposited outside the jet cone, contributions from the underlying event, and energy lost in uninstrumented regions of the detector. The dijet invariant mass, M_{jj} , was computed, and required to be within the range 65 to 110 GeV/c^2 . The background from semileptonic decays of heavy flavors was effectively reduced by discarding events where a Y -decay muon is contained in the cone of a leading jet. The identification of vector bosons in the hadronic final state was hindered by a large contamination from QCD processes, and additional conditions were needed to reduce the background in this channel. We optimized the sensitivity by a kinematic selection which requires $P_T^{\mu\mu} > 14$ GeV/c and $\Delta\phi_{\mu\mu} < 1.4$. While producing a relative decrease of signal acceptance by $\approx 25\%$, these cuts reduce the background-dominated data by a factor of 6.

Dimuon events characterized by one of the four signatures described above were selected as YW^\pm/YZ^0 candidates. A total of 28 events were accepted by the selection; their dimuon invariant mass spectrum is shown in Fig. 3. Three events have dimuon mass in the $Y(1S)$ search window, defined as $9.3 < M_{\mu\mu} < 9.6$ GeV/c^2 . All of them are due to the hadronic identification mode of vector bosons. The acceptance for the $Y(1S)W^\pm/YZ^0$ processes, based on the criteria described above, is reported in Table I. We estimate a SM contribution to our dataset equal to 0.03 and 0.01 signal events from $Y(1S)W^\pm$ and $Y(1S)Z^0$ production, respectively.

Various processes such as $b\bar{b}$, $t\bar{t}$, W/Z , and Drell-Yan $\mu^+\mu^-$ production represent possible background contaminations. However, they are not expected to show any resonant behavior in the $\mu^+\mu^-$ invariant mass spectrum. In Fig. 1 clear $Y(1S)(9460)$ production is evident in the 9.3 to 9.6 GeV/c^2 mass region. Nonresonant behavior is observed in the rest of the spectrum with the exception of the regions 9.85–10.15 GeV/c^2 and 10.2–10.5 GeV/c^2 that are enriched, respectively, with $Y(2S)(10023)$ and $Y(3S)(10355)$ decays. The background evaluations described below are extracted from the non-resonant component of experimental data (in the following simply denoted as “continuum”) and from events with kinematic and identification biases similar to those

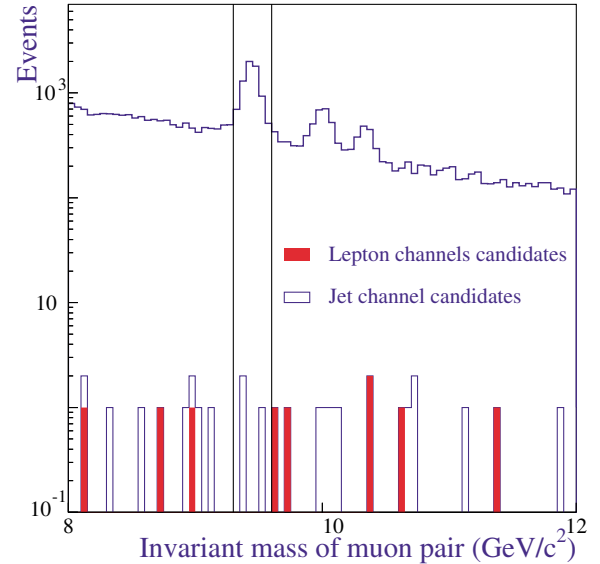


FIG. 3 (color online). Invariant mass of the two muons for events selected in the four search channels; the region within vertical lines defines $Y(1S)W^\pm/Y(1S)Z^0$ candidates. The distribution of all dimuon candidates before the vector boson selection is overlaid.

of signal candidates, for each identification mode of the vector bosons.

The contribution of high- E_T electron events with a dimuon mass in the $Y(1S)$ window is estimated by scaling the number of continuum events with high- E_T electron candidates by the ratio between $Y(1S)$ and continuum computed in a sample containing a “fake electron.” The fake electron is defined as a central $E_T > 20$ GeV jet with a $P_T > 10$ GeV/c track in its cone. The number of expected background events computed is $0.0^{+0.3}_{-0.0}$.

A similar method is used for the background evaluation in the muon channel. Events containing nonmuon tracks with $P_T > 20$ GeV/c are counted in the $Y(1S)$ and continuum regions, and their ratio is used to extrapolate the number of continuum events with high- P_T muon candidates to the $Y(1S)$ window. The number of expected background events computed is $0.0^{+0.6}_{-0.0}$.

In the sample of events with \cancel{E}_T significance, $s > 3$, the number of background events in the $Y(1S)$ window is estimated by rescaling the number of continuum events by the ratio between $Y(1S)$ and continuum computed in an orthogonal sample enhanced in fake missing E_T . This sample is defined by selecting events with $s < 3$ and $\cancel{E}_T > 20$ GeV. This results in a background prediction of 1.4 ± 0.8 events.

The main sources of background in the hadronic channel are due to Drell-Yan radiative processes and heavy flavor production with semileptonic decay to muons. These processes show a smooth behavior in the dimuon invariant mass spectrum and in the M_{jj} spectrum. Therefore, the fraction of events with $65 < M_{jj} < 110$ GeV/c^2 is expected to be the same in the $Y(1S)$

TABLE I. Number of events in the data after all cuts and results of acceptance and background estimates.

Channel	Acceptance (%)		Predicted SM signal	Events	
	$Y(1S)W^\pm$	$Y(1S)Z^0$		Predicted background	Observed
$W/Z \rightarrow eX$	0.52 ± 0.05	0.37 ± 0.03	0.006	$0.0^{+0.3}_{-0.0}$	0
$W/Z \rightarrow \mu X$	0.51 ± 0.05	0.38 ± 0.03	0.006	$0.0^{+0.6}_{-0.0}$	0
$W/Z \rightarrow \cancel{E}_T X$	0.64 ± 0.06	0.72 ± 0.06	0.009	1.4 ± 0.8	0
$W/Z \rightarrow jj$	1.34 ± 0.26	1.35 ± 0.20	0.018	2.1 ± 1.2	3
Total	3.01 ± 0.28	2.82 ± 0.21	0.039	$3.5^{+1.6}_{-1.5}$	3

region and in the continuum. With that hypothesis, the expected background contamination in the $Y(1S)W^\pm / Y(1S)Z^0$ channel is 2.1 ± 1.2 events. The estimated and observed numbers of events in the four channels are summarized in Table I, together with the SM acceptance to $Y(1S)W^\pm$ and $Y(1S)Z^0$.

Several systematic effects on the acceptance were estimated. The use of different parton distribution function sets in the generator can change the total acceptance by about 2%. The color-octet contribution to the process is affected by a large uncertainty in this model; its variation produces an uncertainty of 1.9%. The dominant systematic uncertainties in the electron, muon, and \cancel{E}_T channels are detector effects, trigger modeling, and the identification of $Y(1S) \rightarrow \mu^+ \mu^-$ decays. Dimuon acceptance, which includes trigger modeling and lepton identification cuts, carries a total systematic uncertainty of 7.0%, due to the combined uncertainty on the modeling of selection variables. This was estimated by comparing real muons in the data and in the simulation. Another source of uncertainty is the momentum scale of muon tracks, which may affect the acceptance of the dimuon mass window cut. We estimated the size of the uncertainty by varying the scale by the observed difference (0.2%) between measured and true value of the $Y(1S)$ mass in the data. In addition, we estimated a 3.0% systematic uncertainty on the acceptance of the missing E_T cut. The systematic error on the acceptance in the hadronic channel is dominated by the uncertainty on jet energy scale, and is estimated conservatively from a $\pm 10\%$ variation of the

jet energy measurement. The relative contribution of each systematic uncertainty is reported in Table II.

We computed cross section limits for the searched SM processes with a counting experiment by combining the four channels together, accounting for the total expected background of $3.5^{+1.6}_{-1.5}$ events, the estimated acceptance, and the related systematics according to the method described in [9]. The 95% C.L. upper limits obtained are the following:

$$\sigma[p\bar{p} \rightarrow Y(1S)W^\pm + X] \times B[Y(1S) \rightarrow \mu\mu] < 2.3 \text{ pb},$$

$$\sigma[p\bar{p} \rightarrow Y(1S)Z^0 + X] \times B[Y(1S) \rightarrow \mu\mu] < 2.5 \text{ pb}.$$

In conclusion, we have not observed $Y(1S)$ mesons in association with W^\pm or Z^0 bosons. The sensitivity of the CDF experiment in run I is not sufficient to test the SM prediction of [1] for these processes. With the expected run II increase of integrated luminosity and the upgrades of the CDF detector, we expect to achieve a sensitivity sufficient to observe the Y plus vector boson production processes.

We thank the Fermilab staff and the technical staffs of the participating institutions for their vital contributions. This work was supported by the U.S. Department of Energy and National Science Foundation; the Italian Istituto Nazionale di Fisica Nucleare; the Ministry of Education, Science, Sports and Culture of Japan; the Natural Sciences and Engineering Research Council of Canada; the National Science Council of the Republic of China; the Swiss National Science Foundation; the A. P. Sloan Foundation; the Bundesministerium für Bildung und Forschung, Germany; and the Korea Science and Engineering Foundation.

TABLE II. Systematic uncertainties on signal acceptance.

Dimuon acceptance	7.0%
Integrated luminosity	4.1%
$Y(1S)$ mass window	2.7%
PDF	2.0%
Color octet contribution	1.9%
$s > 3$ cut (\cancel{E}_T channel only)	3.0%
Jet energy scale ($W^\pm \rightarrow jj$)	17.2%
Jet energy scale ($Z^0 \rightarrow jj$)	11.7%
Total (e, μ, \cancel{E}_T channels)	9.0%
Total ($W^\pm \rightarrow jj$)	19.2%
Total ($Z^0 \rightarrow jj$)	14.5%

*Visitor.

- [1] E. Braaten, J. Lee, and S. Fleming, Phys. Rev. D **60**, 91501 (1999).
- [2] J. A. Grifols, J. F. Guion, and A. Mendez, Phys. Lett. B **197**, 266 (1987); R.W. Robinett and L. Weinkauff, Mod. Phys. Lett. A **6**, 1575 (1991).
- [3] G. T. Bodwin, E. Braaten, and G. P. Lepage, Phys. Rev. D **51**, 1125 (1995).
- [4] F. Abe *et al.*, Nucl. Instrum. Methods Phys. Res., Sect. A **271**, 387 (1988).

- [5] Pseudorapidity η is defined as $\eta = -\ln[\tan(\theta/2)]$ with θ measured with respect to the incoming proton direction.
- [6] D. Amidei *et al.*, Nucl. Instrum. Methods Phys. Res., Sect. A **350**, 73 (1994); S. Cihangir *et al.*, Nucl. Instrum. Methods Phys. Res., Sect. A **360**, 137 (1995).
- [7] G. Marchesini *et al.*, Comput. Phys. Commun. **67**, 465 (1992).
- [8] For a detailed accounting of lepton selection criteria suitable for the identification of vector boson decays at CDF see, for instance, T. Affolder *et al.*, Phys. Rev. D **64**, 52001 (2001).
- [9] G. Zech, Nucl. Instrum. Methods Phys. Res., Sect. A **277**, 608 (1989); O. Helene, Nucl. Instrum. Methods Phys. Res. **212**, 319 (1983).